

Decreased Surfactant Protein-B Expression and Surfactant Dysfunction in a Murine Model of Acute Lung Injury

Edward P. Ingenito, Rene Mora, Michael Cullivan, Yolanda Marzan, Kathleen Haley, Lena Mark, and Lawrence A. Sonna

Division of Pulmonary and Critical Care Medicine, Brigham and Women's Hospital and Beth Israel Deaconess Medical Center, Boston; and U.S. Army Research Institute of Environmental Medicine, Natick, Massachusetts

This study examines the relationships between inflammation, surfactant protein (SP) expression, surfactant function, and lung physiology in a murine model of acute lung injury (ALI). 129/J mice received aerosolized endotoxin lipopolysaccharide [LPS] daily for up to 96 h to simulate the cytokine release and acute inflammation of ALI. Lung elastance (E_t) and resistance, lavage fluid cell counts, cytokine levels, phospholipid and protein content, and surfactant function were measured. Lavage and lung tissue SP content were determined by Western blot and immunohistochemistry, and tissue messenger RNA (mRNA) levels were assessed by Northern blot and *in situ* hybridization. Tumor necrosis factor- α and neutrophil counts in bronchoalveolar lavage fluid increased within 2 h of LPS exposure, followed by increases in total protein, interleukin (IL)-1 β , IL-6, and interferon- γ . E_t increased within 24 h of LPS exposure and remained abnormal up to 96 h. SP-B protein and mRNA levels were decreased at 24, 48, and 96 h. By contrast, SP-A protein and mRNA levels and SP-C mRNA levels were not reduced. Surfactant dysfunction occurred coincident with changes in SP-B levels. This study demonstrates that lung dysfunction in mice with LPS-ALI corresponds closely with abnormal surfactant function and reduced SP-B expression.

Abnormal surfactant function is thought to play a central role in the evolution of acute lung injury (ALI) (1). Although application of positive airway pressure helps reverse alveolar instability due to surface film dysfunction by acting as a mechanical "stent," high airway pressures may directly injure the lung, resulting in barotrauma and ventilator-related lung injury (2). Ultimately, the restoration of normal interfacial properties is required to affect complete lung healing and recovery.

Several mechanisms have been proposed to account for surfactant dysfunction during acute respiratory distress syndrome (ARDS)/ALI: (1) enzymatic degradation of critical surfactant components by neutrophil proteases and

phospholipases (3, 4); (2) interference with normal surfactant adsorption by serum proteins and nonsurfactant lipids within the inflamed lung (5); (3) modification of surfactant lipid and protein components by reactive oxygen free radicals released from activated neutrophils and macrophages (6); and (4) decreased synthesis and secretion of essential surfactant components during the acute inflammatory process (7, 8).

Although these mechanisms need not be mutually exclusive, recent data from both animal and human studies suggest that reduced levels of critical surfactant apoproteins are present in the ARDS lung and are important in determining surface film dysfunction. Gregory and colleagues have demonstrated that surfactant from patients with ARDS has reduced levels of both surfactant protein (SP)-A and SP-B, as well as abnormal interfacial properties relative to samples from patients without ARDS (9). Levels of surfactant apoproteins are similarly reduced in animal models of ALI (10). Although reductions in both SP-A and SP-B have been reported at various stages of the inflammatory response, available data suggest that reductions in SP-B are likely to have the most profound biophysical and physiologic consequences.

SP-B plays a critical role in promoting adsorption of surface active components to the air-liquid interface as alveolar area increases, and is essential for maintenance of film stability during compression at body temperature (11). Surfactant devoid of SP-B cannot achieve surface tensions less than 20 dynes/cm during compression, and is therefore unable to stabilize alveoli during normal tidal breathing (12).

SP-B levels appear to decrease in ALI, but the pathophysiology which underlies this observation has not been fully characterized. There is a growing body of evidence to suggest that alterations in SP-B expression are, in part, responsible. Tumor necrosis factor (TNF)- α , a cytokine thought to play a key role in modulating initial stages of ALI, decreases the expression of SP-B in cultured alveolar epithelial cells and in fetal lung tissue explants (13). Direct intratracheal instillation of TNF- α in mice has recently been shown to decrease SP-B messenger RNA (mRNA) levels in lung tissue (8). Other cytokines that modulate the innate immune response to lipopolysaccharide (LPS), such as interleukin (IL)-1 β and IL-6, are increased within the alveolar compartment during ALI and could also participate in downregulating apoprotein expression (14, 15). The present study examines the relationships between lung dysfunction, biochemical and cellular indices of inflammation, cytokine levels, surfactant dysfunction, and SP content and expression in a murine model of ALI resulting from endotoxin exposure.

(Received in original form December 20, 2000 and in revised form March 19, 2001)

Address correspondence to: E. P. Ingenito, M.D., Ph.D., Pulmonary and Critical Care Div., Brigham and Women's Hospital, 75 Francis St., Boston, MA 02115. E-mail: eingenito@partners.org

Abbreviations: acute lung injury, ALI; acute respiratory distress syndrome, ARDS; bronchoalveolar lavage fluid, BALF; complementary DNA, cDNA; lung elastance, E_t ; glyceraldehyde-3-phosphate dehydrogenase, GAPDH; equilibrium surface tension, γ_{equil} ; maximum surface tension during dynamic expansion, γ_{max} ; minimum surface tension during dynamic compression, γ_{min} ; interferon, IFN; interleukin IL; kilobase pairs, kbp; large aggregate PL, LAPL; lipopolysaccharide, LPS; messenger RNA, mRNA; phosphate-buffered saline, PBS; phospholipid, PL; lung resistance, R_t ; sodium dodecyl sulfate, SDS; surfactant protein, SP; saline (or standard) sodium citrate, SSC; tumor necrosis factor, TNF; total protein, TP.

Am. J. Respir. Cell Mol. Biol. Vol. 25, pp. 35-44, 2001
Internet address: www.atsjournals.org

Materials and Methods

Experimental Protocol

All mice were studied in accordance with an experimental protocol approved by our institution's Animal Studies committee. Animals were maintained in a virus-free facility and were studied 1 and 3 wk after delivery from the supplier (6 to 8 wk of age). A total of 42 strain 129/J mice (Jackson Laboratories, Bar Harbor, ME) weighing 18.8 ± 2.1 g (16 to 24 g) were divided into six groups: (1) control animals studied at baseline ($n = 7$); (2) animals exposed to endotoxin (Pseudomonas Serotype 10, Sigma Chemical Co., St. Louis, MO; cat. #L9143) 2 h before study (2 h LPS, $n = 7$); (3) animals exposed to endotoxin 12 h before study (12 h LPS, $n = 7$); (4) animals exposed 24 h before study (24 h LPS, $n = 7$); (5) animals exposed twice, at 24 and 48 h before study (48 h LPS, $n = 7$); and (6) animals exposed four times, at 24, 48, 72, and 96 h before study (96 h LPS, $n = 7$). There were no significant differences in body weights among the groups ($P = 0.37$ by one-way analysis of variance [ANOVA]).

Endotoxin was prepared as an aqueous suspension of 10 mg in 3 ml of normal saline and sonicated for 30 s using a microtip sonicator before dosing (Model W-375; Branson Instruments, Seattle, WA). Administration was performed over a 15-min period in a nebulization chamber using a DeVilbiss nebulizer and continuous airflow of 6 liters/min. After appropriate incubation (2 to 96 h), each animal's lung physiology was measured by forced oscillatory ventilation and each one underwent whole-lung lavage. Lungs were then removed *en bloc* and either were processed for total RNA extraction or were preserved for histopathology, immunohistochemistry, and *in situ* hybridization. Cells were removed from bronchoalveolar lavage fluid (BALF) by low-speed centrifugation, and the resulting pellets were analyzed for total cell and differential counts. Cell-free lavage fluid was stored under nitrogen at -70°C , and subsequently processed for surfactant isolation, total protein (TP) and phospholipid (PL) determinations, cytokine levels, and SP-B and SP-A levels by Western blot analysis.

Measurement of Lung Mechanics

Animals were anesthetized with intraperitoneal pentobarbital (50 mg/kg), and had a tracheal cannula placed. Before the initiation of mechanical ventilation, animal lungs were inflated once to 0.75 ml to ensure that all measurements were initiated with a similar volume history. Ventilator support was administered using 0.3 ml tidal volume, 150 breaths/min, and $\text{FiO}_2 = 0.21$ (room air) with no positive end-expiratory pressure (PEEP) (to simulate conditions of spontaneous breathing) using a computer-controlled, volume-cycled, small animal ventilator (Flexivent; SCIREQ, Montreal, PQ, Canada).

Measurements of lung function were performed using the optimal ventilator waveform method of Lutchen and associates (16): a forced oscillatory volume waveform, with energy at multiple frequencies, was applied as an input signal, and transpulmonary pressure was measured as the dependent output variable. The forcing frequencies and amplitudes were selected to provide effective tidal ventilation while simultaneously allowing the assessment of impedance information over a range of frequencies. This approach allows measurements to be made that are minimally affected by nonlinear mechanics, volume-dependent differences in recoil, or turbulent flows. Low-frequency responses provide specific information about the tissue component of lung resistance, high-frequency responses allow for accurate assessment of airway resistance, and the pattern of change in elastance with frequency provides information about heterogeneity of time constants within the lung. Measurements of lung mechanics were performed in triplicate, and lung resistance and dynamic elastance are expressed as functions of frequency.

Processing of BALF for Cell Counts and Surfactant Isolation

Cells were removed from lung lavage fluid by low-speed centrifugation ($400 \times g$, 4°C , 10 min), and the cell-free supernatant was stored under nitrogen at -70°C . Recovery of instilled lavage fluid averaged 94% (2.82 ± 0.1 ml out of 3) and was not significantly different among the six study groups.

Red-cell lysis was performed using hypotonic buffer (0.1% NH_4Cl), and total white-cell numbers were determined by manual counting. Cell pellets were prepared by centrifugation, stained with Wright's stain, and examined under light microscopy for determination of differential counts.

Surfactant pellets were isolated from cell-free lavage fluid by ultracentrifugation ($60,000 \times g$, 4°C , 45 min). Pellets were resuspended in 250 μl of 0.02% sodium azide/normal saline and stored under nitrogen at -70°C for subsequent PL determination, Western blot analysis, and functional studies. The supernatant remaining after ultracentrifugation was stored at -70°C for protein, PL, and cytokine analysis.

PL and TP Determinations

Total PL determinations were performed according to the method of Stewart (17). TP determinations were performed using the bicinchoninic acid microassay method (Pierce Chemical, Rockford, IL). Measurements were performed separately on surfactant pellets and ultracentrifuge supernatants, and total content for each lavage sample was determined as the sum of results from each determination. Large aggregate PL (LAPL) (18), representing the fraction of total PL specifically associated with intact surfactant, was defined as that present within the centrifuged pellet.

Determination of Static and Dynamic Interfacial Properties of Surfactant Films

Surfactant function was assayed *in vitro* at uniform bulk concentration (1 mg/ml PL content) by pulsating bubble surfactometry (Electronics, Amherst, NY). Samples were loaded according to the modified method of Putz and coworkers (19), in which the open end of the capillary tube is occluded using putty to prevent coating of the tube with surfactant and leakage during oscillations. Leakage was further minimized by injecting air down the capillary tube after bubble formation to push fluid back into the bulk phase and dry the tube.

Samples containing 1.0 mg/ml of total PL in 0.15 M NaCl containing 5 mM CaCl_2 were prepared, and lipid was dispersed by repeated injection through a 27-gauge needle. Measurements of surface tension versus surface area were recorded for samples from LPS-exposed and control animals. Equilibrium surface tensions were measured without oscillations for 15 min. Recordings were then made at 20 cycles/min, 37°C , between $r_{\min} = 0.31$ and $r_{\max} = 0.50$ until stable readings (unchanging over 5 min) were achieved. Static and dynamic calibrations were performed before and after each run using distilled water. Results are reported as γ_{equil} (equilibrium surface tension), γ_{\min} (minimum surface tension during dynamic compression), and γ_{\max} (maximum surface tension during dynamic expansion), and representative dynamic γ -versus-surface area loops are presented.

Lavage Fluid Cytokine Determinations

Levels of TNF- α , IL-1 β , IL-6, IL-10, and interferon (IFN)- γ were determined in BALF surfactant pellets and supernatants using commercially available enzyme-linked immunosorbent assays (Endogen Corp., Cambridge, MA). This panel of cytokines was selected for analysis because it represents those cytokines recognized as being important in modulating the acute innate immune response that follows endotoxin exposure (14). Assays were performed in

duplicate on aqueous surfactant and surfactant ultracentrifuge supernatants (3-fold concentrated) according to manufacturer's instructions without additional processing or purification. Results for each sample represent the average of two determinations.

Western Blot Determinations of SP-A and SP-B in Surfactant Samples

SP-A was purified from calf lung surfactant using a modification of the method of McCormack and colleagues (20). Sample purity was verified by gel electrophoresis, and rabbit antiserum against SP-A was developed for our laboratory (Tana Laboratories, Houston, TX). SP-B was purified by a modification of the method of Beers and associates (21), an approach that renders purified SP-B separate from SP-C. Selective isolation of SP-B was verified by analytical gel electrophoresis performed under nonreducing conditions. This was followed by preparative electrophoresis and protein recovery by electro-elution. This preparation yielded a single band of relative molecular mass = 6,000 by Coomassie brilliant blue-silver staining when examined under reducing conditions, and was used for antisera preparation (Charles River Labs, Needham, MA). Cross-reactivity of SP-A and SP-B antisera raised against bovine apoproteins was demonstrated to murine apoproteins by dot-blotting. SP-A antisera were sensitive to 50 ng of murine SP-A, with no detectable cross-reactivity to SP-B. SP-B antisera were sensitive to 5 ng of murine SP-B, with no detectable cross-reactivity to SP-A. SP-A and SP-B antibodies were both tested against a synthetic full-length SP-C (unpalmitoylated; Tana Labs) that was reconstituted in an acid environment and then neutralized to help promote folding into its native α -helical conformation. Neither antibody cross-reacted with synthetic SP-C.

The quantity of 20 μ g of purified whole surfactant from each mouse surfactant sample was applied to a 15% sodium dodecyl sulfate (SDS) polyacrylamide gel, separated under reducing conditions, and blotted onto a polyvinylidene difluoride membrane. Western blotting was performed in standard fashion, and blots were developed using a streptavidin-biotin peroxidase amplification system (Sigma).

Northern Blot Analysis for SP-A, SP-B, and SP-C

Total RNA was isolated from freshly extracted lungs by guanidinium thiocyanate/phenol/chloroform extraction (Ultraspec RNA reagent from Biotech Labs, Houston, TX; and chloroform from Fisher Scientific, Fair Lawn, NJ). The recovered total RNA was subjected to a second purification step by column chromatography (RNeasy mini-prep kit; Qiagen, Santa Clara, CA) before use. Purity and quantification were determined by absorbance spectrophotometry at 260 and 280 λ .

Complementary DNAs (cDNAs) against SP-A, SP-B, and SP-C for both Northern blot and *in situ* hybridization were prepared from pUC18 and pBluescript SK (ampR) vectors containing cDNA inserts complementary to *Homo sapiens* SP-A (0.844 kilobase pairs [kbp], ATCC #65783), murine SP-C (1.2 kbp, ATCC #711147), and murine SP-B (1.8 kbp, ATCC #263338; American Type Culture Collection, Rockville, MD). The plasmid cDNA inserts were flanked by EcoRI restriction sites. Competent *Escherichia coli* cells (TA Cloning Kit; InVitrogen, Carlsbad, CA) were transformed and single colonies subcultured in LB medium supplemented with ampicillin (100 mg/ml) to produce working stocks containing the transfection vector. Plasmids were purified using the JetStar 2.0 Plasmid MAXI isolation system (PGC Scientific, Frederick, MD). cDNA inserts were cut from the plasmids by EcoRI digestion (New England Biolabs, Beverly, MA), and separated from other digestion products by electrophoresis on a 1.5% agarose gel. cDNA probes were further purified using the QIAquick Gel Extraction Kit (Qiagen). The SP-B insert was

subjected to a second digestion using BamHI (New England Biolabs) to produce 675-base pair (bp) and 1.1-kbp fragments. In preliminary experiments, the 675-bp fragment yielded better hybridization results during Northern blot analysis and was therefore used in all subsequent experiments. cDNA complementary to mouse glyceraldehyde-3-phosphate dehydrogenase GAPDH was purchased directly from Clontech (Palo Alto, CA) for control studies.

The quantity of 20 μ g of total RNA was subjected to electrophoresis in a formaldehyde/1.2% agarose gel, transferred to 0.45 mM pore-size nylon membrane (Schleicher & Schuell, Keene, NH) using 10 \times standard sodium citrate (SSC) as the transfer buffer, and crosslinked to the membrane by ultraviolet exposure. SP-A, SP-B, and SP-C probes were prepared by labeling 50 to 100 ng of cDNA with 32 P, using a Klenow enzyme fragment random primer labeling kit (Boehringer Mannheim, Mannheim, Germany) and α - 32 P-deoxy-adenosine triphosphate (ATP) (New England Nuclear, Boston, MA). The probes were purified before use by passage over NucTrap Probe Purification Columns (Stratagene, La Jolla, CA). To prepare GAPDH probes, 400 ng of cDNA complementary to GAPDH was labeled with 32 P by end-labeling (Boehringer Mannheim) with γ - 32 P-ATP (New England Nuclear). The end-labeled probe was then purified by passage over a NENsorb affinity column (New England Nuclear), and eluted with 50% methanol.

Membranes containing crosslinked RNA were hybridized to 32 P-labeled probes for 2 h at 68°C using ExpressHyb Hybridization Solution (Clontech). The membranes were then washed twice at room temperature in 2 \times SSC/0.05% SDS, once at room temperature in 0.2 \times SSC/0.1% SDS, and once at 50°C in 0.2 \times SSC/0.1% SDS. Northern blots for SP-A, SP-B, SP-C, and GAPDH were performed (sequentially in that order) on the same membrane. Before each subsequent hybridization, probe used for the previous blot was stripped from the membrane by boiling in 10% SDS for 10 min. Autoradiography was performed by exposure to either X-Omat or BioMax film (Kodak, Rochester, NY) at -80°C and the intensity of bands was measured by scanning densitometry.

Immunohistochemistry of Lung Tissue Samples for SP-A and SP-B

Fresh lung tissue was placed in (2%, buffered) paraformaldehyde for 2 h and fixed in 70% histologic grade ethanol, and underwent routine processing for paraffin embedding. From paraffin-embedded samples, 5- μ m sections were cut, immersed in several changes of xylene, rehydrated in graded alcohols, and washed in phosphate-buffered saline (PBS). Primary rabbit polyclonal antisera included anti-SP-B, anti-SP-A, and anti-Clara cell CC10. The antisera for surfactant apoproteins required trypsin pretreatment. Slides were blocked in a 10% solution of rabbit serum in PBS containing 2% bovine serum albumin. After blocking, the primary antibody was applied to slides and slides were incubated overnight at 4°C. Slides were then washed and incubated in the biotinylated secondary antibody for 2 h at 4°C; for this incubation, secondary antibody was diluted 1:200 in 5% dry milk in PBS with 5 μ l/ml murine serum.

After methanol incubation, the avidin-biotin complex (ABC) standard (Vector Laboratories, Carpinteria, CA) was applied and slides were incubated for 1 h at room temperature. Slides were finally developed using 0.025% diaminobenzidine (Sigma) in PBS with 0.1% H₂O₂. The antisera for surfactant apoprotein B required additional amplification after the ABC standard. SP-B slides were washed and then incubated for 6.5 min in biotinylated tyramide (NEN Life Sciences, Boston, MA) followed by a 30-min incubation in streptavidin-horseradish peroxidase (NEN). After these two incubations, SP-B samples were developed as outlined earlier.

In Situ Hybridization for SP-A and SP-B

Biotinylated probes were prepared using the BioPrime DNA labeling kit (GIBCO BRL, Gaithersburg, MD); 1 μ l RNAsin (GIBCO BRL) was added to each probe reaction. Paraffin-embedded tissue sections were immersed in several changes of xylene, rehydrated using graded alcohols, and washed in diethylpyrocarbonate (DEPC)-PBS. Slides were then incubated in 40 μ g/ml proteinase K (GIBCO BRL) for 10 min at 37°C, washed in DEPC-PBS, and incubated for 3 min in 4% paraformaldehyde. Samples were washed in DEPC-PBS, dehydrated through graded alcohols, and air-dried. Probes were diluted 1:25 in the 2 \times hybridization buffer in the *In Situ* Hybridization and Detection System (ISH Kit) (GIBCO BRL) and then 1:1 in 20% dextran, and applied to the slides. Probe was incubated overnight at 42°C. After hybridization, slides were incubated in high-stringency saline sodium citrate (SSC) washes: two washes in 2 \times SSC at room temperature, two washes in 0.2 \times SSC with 0.1% SDS at 42°C, three washes in 0.2 SSC at 42°C, and two final washes in 2 \times SSC. Next, blocking solution was applied and slides were incubated at room temperature for 15 min. The streptavidin-alkaline phosphatase conjugate from the ISH Kit was applied and incubated for 15 min

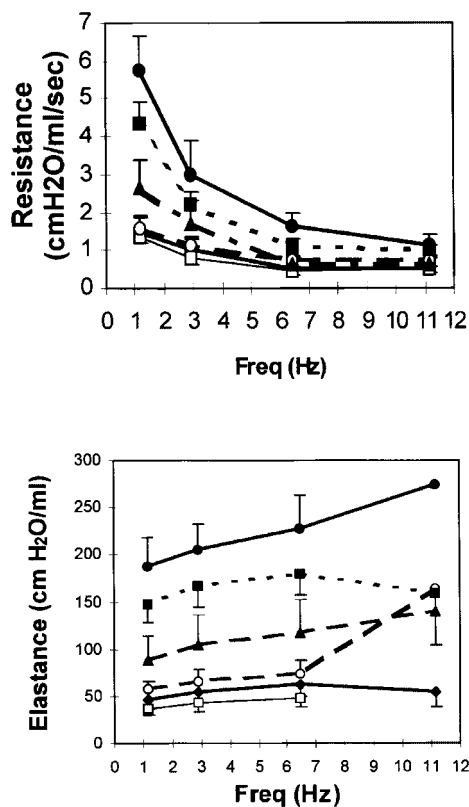


Figure 1. Lung mechanics versus time after LPS exposure. (a) summarizes total lung resistance as a function of frequency for the various treatment groups. At higher frequencies, lung resistance plateaus at a value equal to airway resistance. The frequency-dependent portion of airway resistance, most prominent at lower frequencies, includes heterogeneous airway opening and closing as well as R_L effects. (b) summarizes dynamic elastance as a function of frequency. Treatment groups are as follows: filled diamonds, control; open squares, 2 h; open circles, 12 h; filled triangles, 24 h; filled circles, 48 h; filled squares, 96 h. The results indicate that peak dysfunction is present in 48-h LPS mice, reflected by a marked elevation in lung resistance and dynamic elastance.

at room temperature. Slides were washed in Tris-buffered saline and alkaline substrate buffer (100 mM Tris base, 150 mM NaCl, and 50 mM MgCl₂ hexahydrate). This was followed by a 5-min incubation with 200 μ g/ml levamisole (Sigma) diluted in the alkaline substrate buffer. Slides were then incubated in nitroblue tetrazolium and 5-bromo-4-chloro-3-indolyl-phosphate from the ISH Kit at 37°C until the positive control slides from the ISH Kit demonstrated a deep purple color. Counterstaining was performed using 2% methyl green (Sigma).

Statistical Analysis

Comparison of results between different groups was performed by one-way ANOVA (StatMost Software, Salt Lake City, UT) except where otherwise indicated. Results for each group are summarized as mean values \pm standard deviation except where otherwise indicated. Statistical significance was defined as $P < 0.05$.

Results

In Vivo Lung Mechanics

Lung function expressed as tissue resistance (R_L) and lung elastance (E_L) versus frequency for control and 2-, 12-, 24-, 48-, and 96-h LPS animals ventilated at 0 PEEP is summarized in Figure 1. In control animals, airway resistance was 0.52 ± 0.05 cm H₂O/ml/s, whereas tissue resistance at normal murine breathing frequency (approximately 150 breaths/min) was 0.50 ± 0.21 cm H₂O/ml/s. Dynamic elastance (at 150 breaths/min) was 55.3 ± 11.7 cm H₂O/ml with little frequency-dependent variation apparent at higher frequencies. By 24 h after LPS exposure, significant increases in R_L , airway resistance, and E_L were observed. Peak dysfunction was noted at 48 h, when airway and tissue resistance at 150 breaths/min were increased 98 and 378%, respectively, and E_L was 375% above controls. There was a small, statistically significant improvement in all three physiologic parameters by 96 h, although all three remained markedly abnormal relative to controls.

BALF Cell Counts and Differentials

Cell count and differential results are summarized in Figure 2. At baseline, $97 \pm 2\%$ of alveolar cells were macrophages, and total cells equaled $0.29 \pm 0.07 \times 10^5$ cells/ml. Within 2 h of LPS exposure a marked increase in total cells occurred ($3.7 \pm 1.1 \times 10^5$ cells/ml), due principally to an influx of neutrophils. Total cells ($16.3 \pm 5.3 \times 10^5$ cells/ml) and polymorphonuclear leukocytes (93%) continued to increase progressively for up to 12 h, after which time both

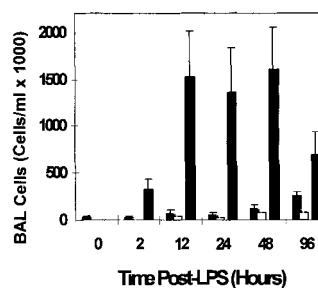


Figure 2. BALF cell counts versus time after LPS exposure. Shaded bars, macrophages; open bars, lymphocytes; filled bars, neutrophils. As early as 2 h after LPS exposure, neutrophils increased significantly within the alveolar compartment. Neutrophils continued to increase until 12 h and then remained unchanged with continued daily

LPS exposure until 96 h, at which time their numbers began to fall. The absolute numbers of macrophages and lymphocytes increased at 48 and 96 h with LPS exposure. Eosinophils were not detected in the BALF at any of the time points examined.

remained elevated but unchanged until 48 h. By 96 h, cell counts and profiles had changed again despite daily LPS exposure. A decrease in total cells, with an increase in percentage of mononuclear cells, was observed.

BALF TP and PL Content

BALF TP and PL contents, determined as the sum of amounts recovered in surfactant pellets and supernatants, are summarized in Figure 3a. LAPL, representing that specifically associated with surfactant, is also shown. Total protein concentrations were unchanged relative to baseline for up to 12 h after LPS exposure but were increased above baseline by 24 h. Protein levels continued to rise with serial LPS administration for up to 96 h, reaching a peak that was 14.7-fold greater than control levels. In contrast, total PL content, as well as surfactant-associated PL, decreased progressively with continued LPS exposure. The most marked reductions were observed in 96-h samples, when LAPL levels reached a nadir of 13% of controls. The effects of LPS exposure on BALF total protein

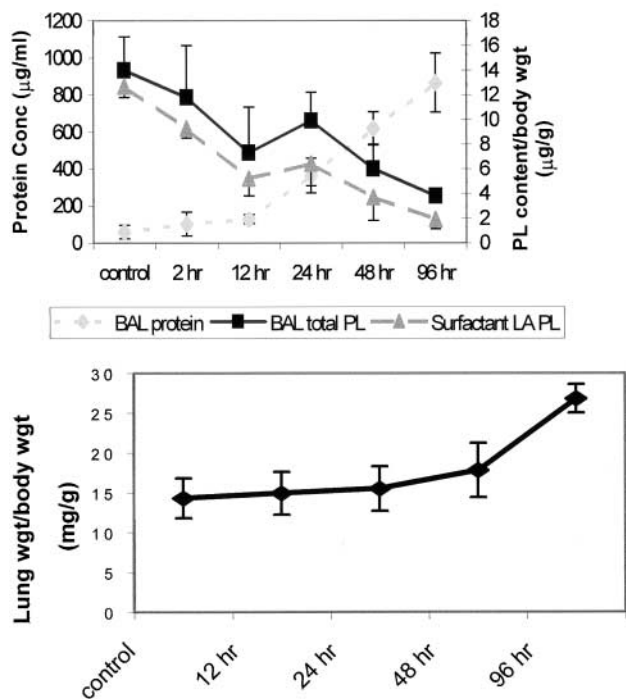


Figure 3. (a) summarizes BALF protein (diamonds), total PL (squares), and large aggregate surfactant PL (triangles) versus time after LPS exposure during the course of the study. BALF protein levels continued to rise with sequential LPS exposures. BALF PL levels decreased with sequential LPS exposures. The large aggregate fraction, which represents intact “high density” surfactant, initially comprised 85% of the total PL fraction. After four doses of inhaled LPS, total PL levels decreased significantly and large aggregate surfactant represented only 46% of the total. (b) summarizes lung weight/total body weight ratio versus time after LPS exposure. Results correlate closely with BALF protein concentration, showing that lung weight increases with serial LPS exposures, likely due to capillary leakage and the development of pulmonary edema.

and PL content together resulted in a large change in the BALF TP/PL ratio. TP/PL was 4.2 ($\mu\text{g protein} \cdot \text{g body weight}/\mu\text{g PL} \cdot \text{ml BALF}$) at baseline, but increased 54-fold to a value of 227.6 ($\mu\text{g protein} \cdot \text{g body weight}/\mu\text{g PL} \cdot \text{ml BALF}$) in 96-h animals.

Lung weight/body weight ratios demonstrated a similar pattern of progressive increase with time in response to LPS exposure (Figure 3b). Significant increases were observed by 48 h, and were maximal at 96-h.

Surfactant Function by Pulsating Bubble Surfactometry

All samples were studied at a uniform concentration of 1 mg/ml PL in 5 mM CaCl_2 . Representative profiles for control and 24-, 48-, and 96-h LPS animals are shown in Figures 4a, 4b, 4c and 4d, respectively. Results, summarized as γ_{min} , γ_{max} , and γ_{equil} , are shown in Table 1. γ_{equil} for control mouse surfactant (24 ± 1.4 dynes/cm) was similar to that previously reported for other species (22). Values of γ_{equil} were similar to those of controls for mice exposed to a single dose of LPS studied at 2, 12, and 24 h, but were elevated relative to controls in multiply-exposed animals at 48 (36.1 ± 8.6 dynes/cm) and 96 (29.6 ± 8.8 dynes/cm) h. The observed time to reach γ_{equil} varied among samples ranging from seconds (in controls) to 30 min (in 48- and 96-h samples).

Dynamic surfactant behavior was markedly different after the different exposures. γ_{min} s during film compression were < 5 dynes/cm in control samples, and remained so at 2 and 12 h after LPS exposure. By 24 h LPS exposure, both γ_{min} and γ_{max} were significantly elevated and remained so at 48 and 96 h. γ_{min} s at 48 and 96 h were approximately 20 dynes/cm, whereas γ_{max} s observed during film

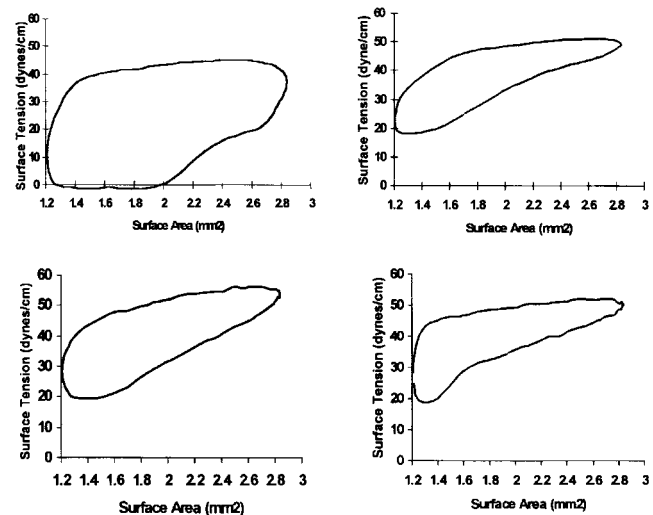


Figure 4. Surfactant function versus time after LPS exposure, as assessed by pulsating bubble surfactometry. Surfactant was diluted in normal saline plus 5 mM CaCl_2 to a final concentration of 1 mg/ml and tested at 20 cycles/min, 37°C . (a) summarizes results for control mouse surfactant. γ_{min} , achieved after 45% compression, is < 1 dyne/cm. (b) shows a representative sample from a 24-h LPS mouse. γ_{min} is markedly elevated, and film hysteresis, reflecting the ability to absorb rapidly after squeeze-out, is markedly diminished. Samples corresponding to 48-h (c) and 96-h LPS exposures (d) show similar surface tension surface area profiles.

TABLE 1

Surfactant characteristics versus time after LPS exposure

Treatment Group	γ_{equil} (dynes/cm)	γ_{min} (dynes/cm)	γ_{max} (dynes/cm)
Control	24.00 ± 1.44	2.00 ± 1.73	39.60 ± 5.32
2-h LPS	24.25 ± 1.07	0.00 ± 0.00	38.00 ± 4.24
12-h LPS	23.50 ± 1.80	3.72 ± 6.41	45.00 ± 7.20
24-h LPS	24.61 ± 0.71	15.46 ± 4.52	49.28 ± 9.77
48-h LPS	36.10 ± 8.65	19.46 ± 1.79	56.76 ± 5.84
96-h LPS	29.63 ± 8.80	19.50 ± 0.71	55.00 ± 1.78

expansion were 55 to 60 dynes/cm. Examination of surface tension versus surface area profiles demonstrated subtle changes in dynamic behavior as early as 12 h after LPS exposure. Increased compression was required to reach γ_{min} by 12 h compared with control and 2-h samples. By 24 h, squeeze-out was noted at 20 dynes/cm in most samples (Figure 4b), with marked elevation in γ_{max} during film expansion and significant loss of film hysteresis. Similar behavior is evident in 48- and 96-h samples (Figures 4c and 4d).

BALF Cytokine Levels: TNF- α , IL-1 β , IL-6, IL-10, and IFN- γ

Cytokine levels were initially measured in both surfactant supernatant and surfactant pellet samples. Virtually no cytokines were detected in the surfactant lipid pellets during initial evaluation, and subsequent analysis was restricted to surfactant supernatants. Results are summarized in Table 2.

TNF- α levels reached maximum values at 2 h after LPS exposure and returned to baseline control levels by 24 h. Levels were undetectable at 48- and 96-h time points, similar to those observed at 24 h. IL-6 levels also rose rapidly after LPS exposure, reaching near-maximal levels by 2 h. In contrast to TNF- α , IL-6 levels remained at or near peak values up to 96 h. IL-1 β increased more gradually. Levels were significantly elevated by 12 h after LPS exposure, peaked at 48 h, and declined toward baseline by 96 h, although remaining significantly elevated compared with controls. IFN- γ and IL-10 demonstrated similar profiles in BALF after LPS exposure, rising gradually and reaching a maximum at 96 h.

Western Blot Analysis of Surfactant Samples and Tissue Immunoperoxidase Staining for SP-A and SP-B

Western blot analysis of surfactant pellets for SP-A and SP-B normalized to PL content are summarized in Figure 5. Results for samples containing 20 μg of surfactant lipid

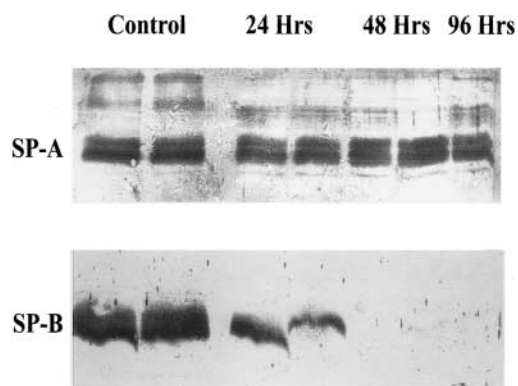


Figure 5. BALF SP-A and SP-B content by Western blot versus time after LPS exposure. Conditions for electrophoresis and Western blot are as described in MATERIALS AND METHODS. Equal amounts of surfactant (20 μg total PL) were loaded onto each lane for the initial electrophoretic separation. SP-A levels did not change with serial exposures to LPS. By contrast, SP-B levels decreased steadily and were minimally detectable at 48 and 96 h.

are shown. SP-B levels were reduced at 24 h, and continued to decline for up to 96 h after LPS exposure. In contrast, SP-A levels (duplicate blots shown) appeared either stable or increased compared with control samples.

These findings are consistent with the results of immunoperoxidase staining observed in lung tissue. Compared with controls (Figure 6), there was a significant decrease in SP-B alveolar immunoperoxidase staining at 96 h. The decrease in staining appeared to occur specifically in alveolar epithelial cells and bronchiolar cells. Immunoperoxidase staining for SP-A showed a distinct pattern with more subtle qualitative, rather than clear quantitative, changes. After LPS exposure, SP-A staining within bronchiolar epithelial cells appeared to be decreased while staining within the extracellular alveolar compartment was increased, suggesting an increase in extracellular SP-A aggregates in the lung periphery.

A potential role for the decrease in SP-B as a determinant of surfactant dysfunction after LPS exposure is most convincingly demonstrated by considering the effects of the addition of 3% (wt/wt) purified bovine SP-B/C mixture on surfactant function. Addition of this mixture of hydrophobic apoproteins restored interfacial properties to nearly normal, with reductions of γ_{min} from 20 dynes/cm to < 3 dynes/cm (Figure 7). These reconstituted samples also demonstrated significantly greater surface tension/surface area hysteresis during dynamic cycling than did those measured before SP-B/C addition.

TABLE 2

BALF cytokine level versus time after LPS exposure

Treatment Group	Cytokine Concentration (pg/ml)				
	TNF- γ	IL-6	IL-1 β	IFN- γ	IL-10
Control	14 ± 6	0	19 ± 5	0	93 ± 18
2-h LPS	16,043 ± 1,373	15,475 ± 242	87 ± 32	0	203 ± 51
12-h LPS	1,783 ± 322	16,317 ± 808	618 ± 44	2,992 ± 813	341 ± 241
24-h LPS	179 ± 91	18,244 ± 318	491 ± 36	3,300 ± 633	323 ± 24
48-h LPS	170 ± 88	18,657 ± 55	1,288 ± 179	9,090 ± 1,322	279 ± 27
96-h LPS	0	14,481 ± 1,573	750 ± 165	14,728 ± 2,774	983 ± 195

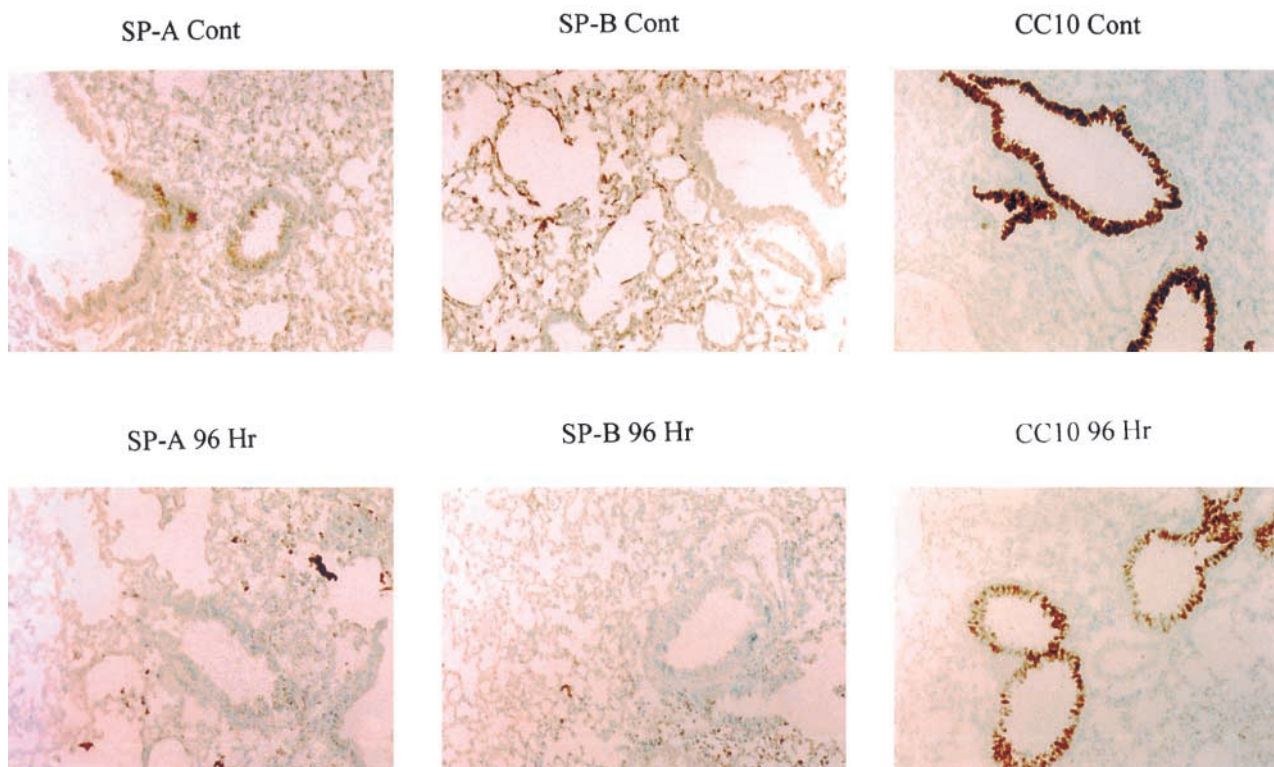


Figure 6. Immunohistochemical characterization of tissue levels and distribution of SP-A, SP-B, and CC-10 (a control protein) in lungs from untreated control mice and mice in the 96-h LPS treatment group. Control tissues show SP-A present in both alveolar epithelial and bronchiolar cells (*left upper panel*), SP-B most prominent in alveolar epithelial cells (*middle upper panel*), and CC-10 (*right upper panel*) exclusively in bronchiolar cells. After LPS exposure, SP-A is present as aggregates within the parenchyma and extracellular compartment (*left lower panel*), SP-B is markedly reduced within the alveolar epithelium (*middle lower panel*), and CC-10 (*right lower panel*) is moderately reduced in bronchiolar epithelial cells.

Northern Blot Analysis and *In Situ* Hybridization

Northern blot analysis for SP-B, SP-A, SP-C, and GAPDH were performed on six samples at each time point. Two separate membranes were prepared; results from one example are shown in Figure 8. SP-B RNA levels in lung tissue were decreased by 24 h and remained depressed relative to controls for up to 96 h, whereas SP-A and SP-C RNA levels appeared unchanged or increased slightly at 24 to 48 h and returned to near baseline by 96 h. Densitometry results, expressed as percentage changes relative to the housekeeping gene GAPDH, showed reductions in SP-B of $63 \pm 22\%$, $78 \pm 9\%$, and $71 \pm 13\%$ at 24, 48, and 96 h, respectively. SP-A and SP-C mRNA levels increased 1.7- and 1.3-fold, respectively, at 24 h, but were nearly equivalent to control levels at 48 and 96 h after LPS exposure.

Reductions in SP-B observed by Northern blot analysis were supported by findings of *in situ* hybridization (Figure 9). A decrease in staining for SP-B RNA within alveolar epithelial cells was observed after LPS exposure relative to control samples.

Discussion

The present study examines the relationship between lung inflammation and physiology, and the surfactant interfacial properties and apoprotein composition during the de-

velopment and progression of acute lung injury. Its primary objective was to characterize the biochemical and molecular mechanisms that underlie surfactant dysfunction in ARDS. Results presented here demonstrate that alterations in lung function *in vivo* correlate closely with the development of surfactant dysfunction *in vitro*. They further demonstrate that dysfunction relates to specific changes in surfactant composition: (1) increased TP relative to surfactant PL content; and (2) decreased SP-B content. Changes in SP-B levels observed by Western blot and immunohistochemistry appear to correlate with decreased SP-B mRNA levels by both Northern blot and *in situ* hybridization. By contrast, levels for SP-A and SP-C mRNA were either increased or unchanged after LPS exposure.

The physiologic changes that followed LPS exposure in this murine model are consistent with those observed in ALI/ARDS. Statistically significant increases in the magnitude of R_L and E_L were noted at 24, 48, and 96 h, suggesting that abnormal physiology resulted primarily from effects of inflammation on the mechanical properties of the lung parenchyma rather than the airways. The frequency dependence observed in E_L between 1 and 18 Hz is most consistent with the presence of heterogeneity. At 24, 48, and 96 h, increasing frequency dependence of E_L was observed, favoring the presence of a multiple time-constant system. If homogeneous dysfunction had accounted for

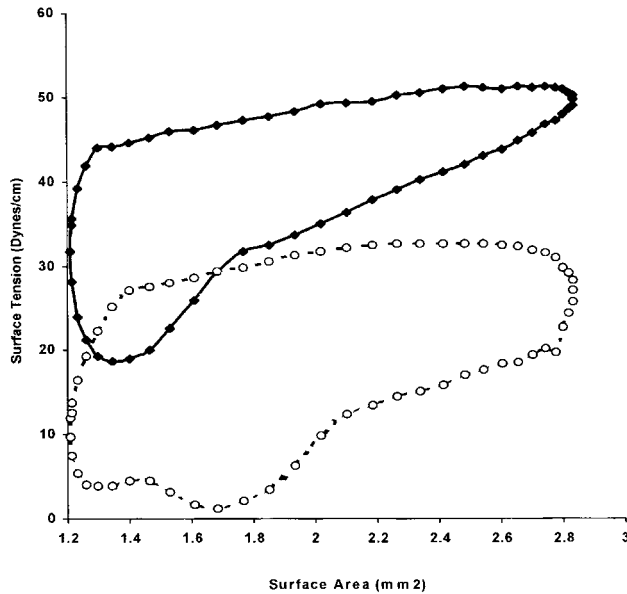


Figure 7. Effect of SP-B replacement on surfactometry of 96-h LPS-exposed surfactant. Surface tension-versus-surface area profiles for 96-h LPS surfactant (*filled diamonds*) and for 96-h LPS surfactant after the addition of 3% (wt/wt) purified bovine SP-B/C (*open circles*) are shown. Surfactant from 96-h LPS animals before addition of SP-B/C shows elevated γ_{\min} (20 dynes/cm) and reduced hysteresis. After addition of the hydrophobic SPs, γ_{\min} returned toward normal and surface film hysteresis was markedly increased. The profile appears similar to that of the control murine surfactant shown in Figure 4a.

the observed changes in lung mechanics, elastance would have increased uniformly at all frequencies without obvious frequency-dependent differences compared with controls (23).

Surfactant function assessed *in vitro* correlated closely with lung function measured *in vivo*. At baseline, murine surfactant functioned similarly to control guinea pig surfactant and calf lung surfactant (22, 24). At 2 h after LPS

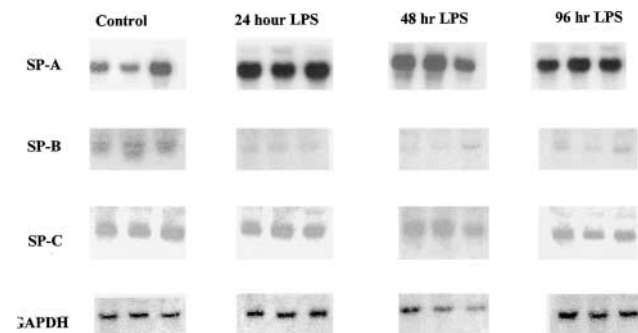


Figure 8. Northern blot analysis of total RNA extracted from lung tissue from mice in the control and 24, 48, and 96-h LPS treatment groups for SP-A, SP-B, SP-C, and GAPDH (control gene) mRNA. SP-B mRNA levels steadily declined after LPS exposure. SP-A and SP-C actually increased initially after LPS exposure and remained above or at control levels despite LPS exposure. GAPDH was unaffected by LPS exposure.

exposure, function remained indistinguishable from controls. By 12 h, dynamic surfactant function was significantly abnormal, although γ_{equil} s were not different from controls, and γ_{\min} s still reached values < 1 dyne/cm during film compression. However, a much greater degree of film compression was required to reach γ_{\min} than at baseline.

At 24 h after LPS exposure, γ_{\min} s were significantly abnormal and the potential for adverse physiologic consequences was readily appreciated. Surface tension/surface area profiles (Figure 4b) demonstrated γ_{\min} s of 20 dynes/cm, γ_{\max} s of 50 to 60 dynes/cm, and markedly reduced surface tension/surface area hysteresis. Dynamic behavior of surfactant samples from 48- and 96-h animals (Figures 4c and 4d) was similar to that observed in 24-h animals.

Surface film dysfunction assessed *in vitro* at uniform bulk concentration after LPS exposure appeared to relate directly to reductions in SP-B levels. At 24 h after LPS exposure, when dynamic film behavior first demonstrated significant increases in γ_{\min} , SP-B was significantly reduced relative to control levels, whereas SP-A appeared to be slightly increased. The physiologic consequences of reduced SP-B levels within the first 24 h after LPS exposure are most convincingly demonstrated by considering the effects of the addition of 3% (wt/wt) purified bovine SP-B/C mixture on surfactant function. Restoration of interfacial properties, as shown in Figure 7, suggests that the majority of dysfunction observed in these samples can be reversed by repletion of the hydrophobic apoprotein components.

These studies do not specifically discriminate between the relative contributions of SP-B and SP-C to functional restoration. However, in combination with Northern blot results showing a marked reduction in SP-B but not SP-C mRNA after LPS exposure, the data suggest that dysfunction may relate specifically to reduced SP-B levels. Together, these observations support the hypothesis that a decrease in SP-B plays a primary role in determining surfactant dysfunction in ALI after LPS exposure. They are consistent with observations from several clinical studies documenting short-term improvement in lung physiology

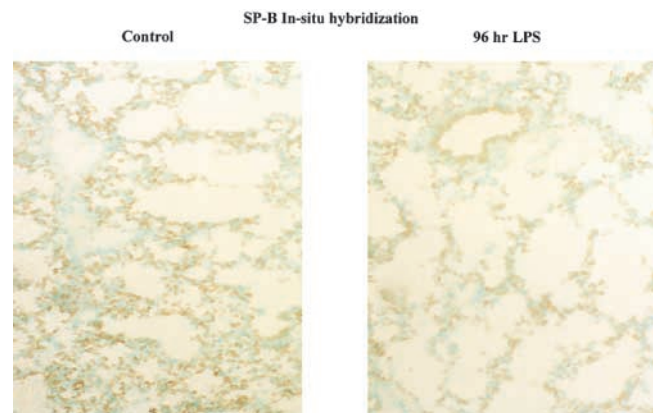


Figure 9. *In situ* hybridization was performed to specifically detect SP-B mRNA. Control samples show normal SP-B with a strong signal at the level of the parenchymal alveolar cell. After serial LPS exposures (96-h sample), SP-B tissue RNA signal was markedly reduced, consistent with Northern blot results.

after addition of surfactant containing SP-B to patients with ARDS (25, 26).

The results further suggest that reduced surfactant SP-B levels observed by Western blot relate (Figure 5), at least in part, to a reduction in SP-B expression by alveolar epithelial cells. Northern blot studies (Figure 8) document a decrease in total lung SP-B mRNA, whereas immunoperoxidase staining on histology specimens (Figure 6) and parallel *in situ* hybridization studies (Figure 9) confirm that the decrease in SP-B protein and RNA resides specifically at the level of the alveolar epithelial cell. Both SP-B protein and SP-B mRNA levels were decreased in 24-, 48-, and 96-h LPS-exposed animals relative to controls. These findings would appear to contrast with the results of Sugahara and associates (27), who demonstrated that intratracheal LPS administration in rats caused an apparent *increase* in alveolar epithelial cell SP-A, SP-B, and SP-C mRNA levels by immunoperoxidase staining and *in situ* hybridization. However, the two studies used very different LPS doses and modes of administration, and analyzed responses at different time points after LPS exposure. The present study specifically examines the direct effects of administration of high doses of LPS targeted toward the lung periphery by nebulization during the first 96-h time period. Sugahara and coworkers examined the delayed, longer term, and indirect effects of low-dose, proximal airway administration of LPS on responses in the lung periphery. This may represent a better model of innate immune system “priming” as opposed to that of ALI, which was the focus of our study. Our results also contrast to the recently reported effects of hyperoxic lung injury on SP-B metabolism in mice. In those studies, hyperoxia appears to promote hypersecretion of SP-B into the alveolar space leading to its depletion at the tissue level (28). By contrast, the widespread lung inflammation produced by nebulized LPS in this study appears to cause a global reduction of SP-B levels and expression within the lung.

Decreases in tissue SP-B cannot be readily explained by a nonspecific reduction in protein expression resulting from diffuse epithelial cell injury or death. SP-A, which is also produced by alveolar cells, was increased on Western blot and by immunoperoxidase staining. Levels of both SP-A and SP-C mRNA were increased within the lung by Northern blot (Figure 8). Such findings suggest that loss of functional epithelial cells does not explain the decrease in SP-B observed here.

These data argue that the observed changes in SP-B are determined partly by pretranslation events. However, they do not discriminate between differences in apoprotein mRNA levels related to altered rates of transcription and differences related to changes in RNA stability. Recent findings examining the effects of cytokines on surfactant apoprotein expression in isolated cell-culture studies suggest both processes may be affected. TNF- α , which increased with 2 h of LPS exposure, has been shown to decrease the expression of SP-B in human pulmonary adenocarcinoma cells by affecting RNA stability, whereas results in fetal tissue explants and reported gene constructs suggest that the rate of SP-B mRNA transcription is also reduced (7, 8).

The pattern of cytokine expression reported here is consistent with that described in the innate immune response

to bacterial infection and includes cytokines that have previously been shown to influence SP-B expression. Although SP-B protein and mRNA levels do decline in association with TNF- α expression, this decline was also associated with increased expression of IL-1 β and IL-6 at 24, 48, and 96 h. The effects of these cytokines on alveolar type II cell SP expression are less well characterized than are the effects of TNF- α , and therefore the pathophysiologic significance of increased IL-1 β and IL-6 levels with respect to altered SP expression remains speculative. Nevertheless, these findings do not preclude the possibility that multiple cytokines are involved in modulating regulation of SP expression during acute lung injury, and that different cytokines may modulate distinct aspects of this response as the syndrome evolves.

Although our results support a central role for decreased SP-B expression in the development of surfactant dysfunction and overall lung dysfunction after LPS exposure, this study does not rule out significant contributions from other mechanisms as well. Our data cannot rule out apoprotein degradation due to neutrophil proteases. In this respect, it is interesting that levels of SP-A, which may be more susceptible to protease degradation than the hydrophobic apoproteins (3), remained flat despite increased levels of SP-A mRNA at 24 and 48 h. Inhibition by serum proteins is also a potential mechanism contributing to dysfunction in samples examined 24, 48, and 96 h after LPS exposure. The effects of exogenous proteins may act synergistically with reduced levels of SP-B to promote dysfunction in this setting (5).

Further, it is clear that this model fails to reproduce the biologic characteristics of human ARDS with respect to BALF SP-A levels. Although we demonstrated reduction in SP-B levels here similar to what has been reported in human studies, decreases in both SP-B and SP-A have previously been observed in patients with ARDS (9). Although the available data do not allow for a complete understanding of why this difference exists, several factors may be important. Results from *in vitro* studies, and from analysis of human samples, suggest that SP-A is susceptible to both free radical-mediated damage and protease degradation in the extracellular environment (3, 6). Samples obtained for SP-A analysis from patients with ARDS have come from individuals with established disease on mechanical ventilator support, presumably receiving high levels of supplemental oxygen. These factors may promote oxidative stress and ventilator-induced lung injury that could alter SP-A levels by the mechanisms not accounted for by the simple LPS exposure model described here. It is also possible that altered SP-A levels in humans with ARDS result in part from a decrease in epithelial cell numbers resulting from widespread apoptosis and necrosis, which the present model does not accurately represent. Differences in SP-A uptake and processing by alveolar epithelial cells and macrophages, as well as differences in amount of SP-A leakage from the alveolar compartment back into the circulation may also contribute to observed differences in lavage fluid levels of this protein (29). Finally, differences in SP-A transcriptional regulation, or mRNA stability, may exist between the human and murine respiratory systems in response to LPS exposure, and

may partly account for the observed differences in SP-A levels reported here compared with what has been observed in ARDS.

Despite these limitations, the murine model of acute lung injury described here displays many of the physiologic, biochemical, and immunologic characteristics of human ARDS. Lung dysfunction is observed in concert with surfactant dysfunction, and is associated with a marked rise in inflammatory cytokines and parallel decrease specifically in SP-B protein and mRNA levels. These findings suggest that altered surfactant function which is associated with LPS-related ALI is in part related to changes in the expression of SP-B, and that treatment strategies directed at increasing SP-B expression may have a role in the future therapy of ARDS.

Acknowledgments: The authors acknowledge the assistance of Dr. Guo-Ping Shi with the preparation of polyclonal antibodies against SP-B. Anti-Clara cell CC-10 antibody was a generous gift of Dr. G. B. Singh. This work was supported by the National Institute of Heart Lung and Blood (HL 33009), the U.S. Army Medical Research and Material Command, and the Beth Israel Deaconess Research Foundation.

References

- Hallman, M., R. Spragg, and J. Harrel. 1982. Evidence of lung surfactant abnormalities in respiratory failure. *J. Clin. Invest.* 70:673-683.
- Dreyfuss, D., P. Soler, and G. Saumon. 1995. Mechanical ventilation-induced pulmonary edema: interactions with previous lung alterations. *Am. J. Respir. Crit. Care Med.* 151:1568-1575.
- Ryan, S. F., Y. Ghassibi, and D. Liau. 1991. Effects of activated polymorphonuclear leukocytes upon pulmonary surfactant in vitro. *Am. J. Respir. Cell Mol. Biol.* 4:33-41.
- Enhorning, G., B. Shumel, L. Keicher, J. Sokolowski, and B. A. Holm. 1992. Phospholipases introduced into the hypophase affect the surfactant film outlining a bubble. *J. Appl. Physiol.* 73:941-945.
- Holm, B. A., G. A. Enhorning, and R. H. Notter. 1998. A biophysical mechanism by which plasma proteins inhibit lung surfactant activity. *Chem. Phys. Lipids* 49:49-55.
- Mark, L., and E. P. Ingenito. 1999. Surfactant function and composition after free radical exposure generated by transition metals. *Am. J. Physiol. (Lung, Cell Mol. Physiol.)* 276:L491-L500.
- Whitsett, J. A., J. C. Clark, J. R. Wispe, and G. S. Pryhuber. 1992. Effects of TNF- α and phorbol ester on human surfactant protein and MnSOD gene transcription in vitro. *Am. J. Physiol. (Lung Cell Mol. Physiol.)* 262:L688-L693.
- Pryhuber, G. S., C. Bachurski, R. Hirsch, A. Bacon, and J. A. Whitsett. 1996. Tumor necrosis factor- α decreases surfactant protein B mRNA in murine lung. *Am. J. Physiol. (Lung Cell Mol. Physiol.)* 270:L714-L721.
- Gregory, T., W. J. Longmore, M. A. Moxley, and J. A. Whitsett. 1991. Surfactant chemical composition and the biophysical activity in the acute respiratory distress syndrome. *J. Clin. Invest.* 88:1976-1981.
- Ingenito, E. P., R. Mora, L. H. Sanna, M. Cullivan, Y. Marzan, and K. Haley. 1999. Reduced SP-B protein and mRNA levels correlate with surfactant dysfunction in a murine model of acute lung injury. *Am. J. Respir. Crit. Care Med.* 159:A159. (Abstr.)
- Ingenito, E. P., L. Mark, J. Morris, F. F. Espinosa, R. D. Kamm, and M. Johnson. 1999. Biophysical characterization of lung surfactant components. *J. Appl. Physiol.* 86:1702-1714.
- Ingenito, E. P., F. F. Espinosa, L. Mark, R. D. Kamm, J. Morris, and M. Johnson. 1997. Contributions of individual surfactant components to adsorption-desorption kinetics and isotherm behavior. *Am. J. Respir. Crit. Care Med.* 155:A211. (Abstr.)
- Wispe, J. R., J. C. Clark, B. B. Warner, D. Fajardo, W. E. Hull, R. B. Holtzman, and J. A. Whitsett. 1990. Tumor necrosis factor alpha inhibits expression of pulmonary surfactant protein. *J. Clin. Invest.* 86:1954-1960.
- Abbas, A. K., A. H. Lichtman, and J. S. Pober. 1997. Cellular and Molecular Immunology, 3rd ed. W. B. Saunders, Philadelphia.
- Bry, K., U. Lappalainen, and M. Hallman. 1996. Cytokines and production of surfactant components. *Semin. Perinatol.* 20:194-205.
- Lutchen, K. R., K. Yang, D. Kaczka, and B. Suki. 1993. Optimal ventilator waveforms for estimating low-frequency respiratory impedance. *J. Appl. Physiol.* 75:478-488.
- Stewart, J. C. M. 1980. Colorimetric determination of phospholipids with ammonium ferrocyanate. *Anal. Biochem.* 104:10-14.
- Ito, Y., R. A. W. Veldhuizen, L. Yao, L. McCaig, A. J. Bartlett, and J. F. Lewis. 1997. Ventilation strategies affect surfactant aggregate conversion in acute lung injury. *Am. J. Respir. Crit. Care Med.* 155:493-499.
- Putz, G., J. Goerke, H. W. Tausch, and J. A. Clements. 1994. Comparison of captive and pulsating bubble surfactometers with use of lung surfactants. *J. Appl. Physiol.* 76:1425-1431.
- McCormack, F. X., H. M. Calvert, P. A. Watson, D. L. Smith, R. J. Mason, and D. R. Voelker. 1994. The structure and function of surfactant protein A. *J. Biol. Chem.* 269:5833-5841.
- Beers, M. F., S. R. Bates, and A. B. Fisher. 1992. Differential extraction for the rapid purification of bovine surfactant protein B. *Am. J. Physiol.* 262:L773-L778.
- Otis, D. R., E. P. Ingenito, R. D. Kamm, and M. Johnson. 1994. Dynamic surface tension of TA surfactant: experiments and theory. *J. Appl. Physiol.* 77:2681-2688.
- Kaczka, D. W., E. P. Ingenito, E. Israel, and K. R. Lutchen. 1999. Airway and lung tissue mechanics in asthma. *Am. J. Respir. Crit. Care Med.* 159:169-178.
- Kennedy, M., D. Phelps, and E. Ingenito. 1997. Mechanisms of Surfactant dysfunction in early acute lung injury. *Exp. Lung Res.* 23:171-189.
- Spragg, R. G., N. Gilliard, P. Richman, R. M. Smith, D. Hite, D. Pappert, B. Robertson, T. Curstedt, and D. Strayer. 1994. Acute effects of a single dose of porcine surfactant on patients with adult respiratory distress syndrome. *Chest* 105:195-202.
- Gregory, T. J., K. P. Steinberg, R. Spragg, J. E. Gadek, T. M. Hyers, W. J. Longmore, M. A. Moxley, G. Z. Cai, R. D. Hite, R. M. Smith, L. D. Hudson, C. Crim, P. Newton, B. R. Mitchell, and A. J. Gold. 1997. Bovine surfactant therapy for patients with acute respiratory distress syndrome. *Am. J. Respir. Crit. Care Med.* 155:1309-1315.
- Sugahara, K., K. Iyama, K. Sano, Y. Kuroki, T. Akino, and M. Matsumoto. 1996. Overexpression of surfactant protein SP-A, SP-B, and SP-C in rats with LPS-induced lung injury. *Lab. Invest.* 74:209-220.
- Tokieda, K., H. S. Iwamoto, C. Bachurski, S. E. Wert, W. M. Hull, K. Ikeda, and J. A. Whitsett. 1999. Surfactant protein-B-deficient mice are susceptible to hyperoxic lung injury. *Am. J. Respir. Cell Mol. Biol.* 21:463-472.
- Doyle, I. R., A. D. Bersten, and T. E. Nicholas. 1997. Surfactant proteins-A and -B are elevated in plasma of patients with acute respiratory failure. *Am. J. Respir. Crit. Care Med.* 156:1217-1229.